

Surface structure of Ce-doped uranium dioxide: SEM, XRD and Raman analysis

Jeongmook Lee^{a*}, Dong Woo Lee^a, Jandee Kim^a, Young-Sang Youn^b, Jong-Yun Kim^{a,c}
and Sang Ho Lim^{a,c}

^aNuclear Chemistry Research Division, Korea Atomic Energy Research Institute,

111 Daedeok-daero 989 Beon-gil, Yuseong-gu, Daejeon, 34057, Republic of Korea

^bDepartment of Chemistry, Yeungnam University, 280 Daehak-ro, Gyeongsan, Gyeongbuk, 38541

^cDepartment of Radiochemistry & Nuclear Nonproliferation, University of Science & Technology,
Gajeong-ro 217, Yuseong-gu, Daejeon, 34113, Republic of Korea

*Corresponding author: leejm@kaeri.re.k

1. Introduction

After irradiation of UO_2 nuclear fuel, fission products (FPs) including lanthanides and activation products are produced and located in the fuel [1-3]. Those fission products could be doped in the nuclear fuel as $(\text{U,FP})\text{O}_{2\pm x}$ form in spent nuclear fuel. Lanthanides doped $\text{UO}_{2\pm x}$ have been studied as simulated spent fuel to understand the structural character of the spent nuclear fuel. Raman spectroscopy has been used to investigate surface structure of the nuclear fuel materials, because of its sensitivity, convenience and non-destructive sample preparation [4]. The Raman studies on trivalent-doped UO_2 directly show the defect due to oxygen vacancy that could be created by loss of oxygen for neutral charge compensation [5-7]. This defect should have significant effect on the kinetics of fuel oxidation.

In this study, we have been investigated the effect on Ce-doping on the UO_2 structure with XRD, SEM and Raman spectroscopy to characterize the defect structure of nuclear fuel material

2. Experimental Section

Ce-doped UO_2 sample pellets with various doping level were prepared by the sintering of a mixture of UO_2 and CeO_2 powders with appropriate compositions. The pelletized powder mixtures were sintered at 1700°C for 18 h in hydrogen atmosphere. After then, those were annealed in same atmosphere at 1200°C for 12 h. The surface structure of the sample pellets was analyzed and characterized using X-ray diffraction (XRD), scanning electron microscopy (SEM) and Raman spectroscopy.

XRD data was collected by Bruker D8 Advance using $\text{CuK}\alpha$ line source (beam current 40mA at 40kV) with 0.02° scan step. The lattice parameters of the samples were calculated from XRD spectra with the refinement process.

Raman spectra were acquired using ANDOR Shamrock SR500i spectrometer with a 633 nm excitation wavelength He-Ne laser. The morphologies of sample surface were also obtained by SEM using 20 keV electron acceleration voltage with 10 mm working distance.

3. Results

The lattice parameters of Ce-doped UO_2 linearly decreased with increasing Ce doping level. This linear relationship was also observed for Gd- and Nd-doped UO_2 , and represented that sample pellets were formed as a solid solution [7,8]. The grain size observed in SEM images of Ce-doped UO_2 decreased as Ce doping level increased. This feature was also similar with Gd- and Nd-doped UO_2 . That change of the grain size should be strongly related to the substituted cation because trivalent cation induce the creation of oxygen vacancy which has smaller apparent radius than that of oxygen.

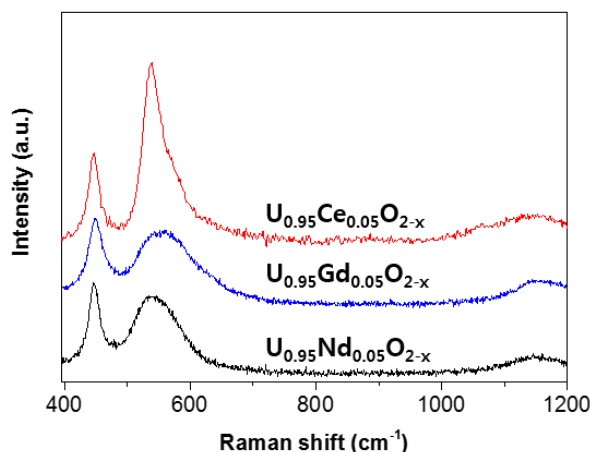


Fig.1. Raman spectra of $\text{U}_{0.95}\text{Nd}_{0.05}\text{O}_{2-x}$ (black line), $\text{U}_{0.95}\text{Gd}_{0.05}\text{O}_{2-x}$ (blue line) and $\text{U}_{0.95}\text{Ce}_{0.05}\text{O}_{2-x}$ (red line) pellets at room temperature, respectively

Raman spectrum of Ce-doped UO_2 sample pallet is shown with those of Gd- and Nd-doped UO_2 in Fig. 1. The peak shown at $\sim 445\text{ cm}^{-1}$ has been assigned to U-O symmetric stretching mode in the fluorite structure [9-11]. Small and broad peak at $\sim 1150\text{ cm}^{-1}$ is ascribed to an overtone of the first order longitudinal optical phonon mode regarded as fingerprint for quasi-perfect fluorite structure [12,13].

The broad peak at $500 \sim 650\text{ cm}^{-1}$ is mainly formed by the peak at $\sim 530\text{ cm}^{-1}$ representing defect due to oxygen vacancy associated with trivalent cation. Gd- and Nd-doped UO_2 have similar intensity of peak at $\sim 530\text{ cm}^{-1}$ for same doping level. It is also known that La-

doped UO_2 with similar doping level showed same features [6]. However, Ce-doped UO_2 shows higher peak intensity at same position although it has same doping level with Gd- and Nd-doped UO_2 . It is expected that Ce doping has a significant influence on defect structure formation by oxygen vacancy. To define this influence, more microscopic analysis technique and ab initio calculation method would be applied.

4. Conclusion

Ce-doped UO_2 with various doping levels were characterized by XRD, SEM and Raman spectroscopy. Ce doping formed the oxygen vacancy and the smaller grain size in UO_2 surface structure like other trivalent doping elements, Gd^{3+} , Nd^{3+} and La^{3+} . However, Ce doping more affected the creation of defect due to oxygen vacancy associated with trivalent cation than Gd, Nd and La doping.

ACKNOWLEDGEMENT

This work was supported by the National Research Foundation of Korea (NRF) grant funded by the Korean government (MSIT) (2017M2A8A5014754)

REFERENCES

- [1] H. Kleykamp, The chemical state of the fission products in oxide fuels, *Journal of Nuclear Materials*, Vol.131, pp. 221-246, 1985.
- [2] R.J.M. Konings, T. Wiss, O. Beneš, Predicting material release during a nuclear reactor accident, *Nature Materials*, Vol.14, pp. 247–252, 2015.
- [3] R.C. Ewing, Long-term storage of spent nuclear fuel, *Nature Materials*, Vol.14, pp. 252–257, 2015.
- [4] M. Schmitt, J. Popp, Raman spectroscopy at the beginning of the twenty-first century, *Journal of Raman Spectroscopy*, Vol.37, pp. 20–28, 2006.
- [5] L. Desgranges, Y. Pontillon, P. Matheron, M. Marcet, P. Simon, G. Guimbretie, et al., Miscibility Gap in the U–Nd–O Phase Diagram: a New Approach of Nuclear Oxides in the Environment?, *Inorganic Chemistry*, Vol.51, pp. 9147–9149, 2012.
- [6] Z. Talip, T. Wiss, P.E. Raison, J. Paillier, D. Manara, J. Somers, et al., Raman and X-ray Studies of Uranium-Lanthanum-Mixed Oxides Before and After Air Oxidation, *Journal of American Ceramic Society*, Vol.98, pp. 2278–2285, 2015.
- [7] J. Lee, J. Kim, Y.-S. Youn, N. Liu, J.-G. Kim, Y.-K. Ha, D. W. Shoemith, and J.-Y. Kim, Raman study on structure of $\text{U}_{1-y}\text{Gd}_y\text{O}_{2-x}$ ($y=0.005, 0.01, 0.03, 0.05$ and 0.1) solid solutions, *Journal of Nuclear Materials*, Vol.486, pp. 216-221, 2017.
- [8] J. Lee, J. Kim, Y.-S. Youn, J.-Y. Kim and S. H. Lim, Surface characterization of $(\text{U,Nd})\text{O}_2$: the influence of trivalent-dopant on structure of UO_2 , *Progress in Nuclear Science and Technology* Vol.5, pp. 33-36, 2018.
- [9] G.C. Allen, I.S. Butler, Characterisation of uranium oxides by micro-Raman spectroscopy, *Journal of Nuclear Materials*, Vol.144, pp. 17–19, 1987.
- [10] P.R. Graves, Raman Microprobe Spectroscopy of Uranium Dioxide Single Crystals and Ion Implanted Polycrystals, *Applied Spectroscopy*, Vol.44, pp. 1665–1667, 1990.
- [11] G.M. Begun, R.G. Haire, W.R. Wilmarth, J.R. Peterson, Raman spectra of some actinide dioxides and of EuF_2 , *Journal of the Less Common Metals*, Vol.162, pp. 129–133, 1990.
- [12] D. Manara, B. Renker, Raman spectra of stoichiometric and hyperstoichiometric uranium dioxide, *Journal of Nuclear Materials*, Vol. 321, pp. 233–237, 2003.
- [13] T. Livneh, E. Sterer, Effect of pressure on the resonant multiphonon Raman scattering in UO_2 , *Physical Review B*, Vol.73, p. 085118, 2006.